

# ZMPSTE24 Regulates SARS-CoV-2 Spike Protein–enhanced Expression of Endothelial PAI-1

Mingming Han<sup>1,2</sup> and Deepesh Pandey<sup>1</sup>

<sup>1</sup>Department of Anesthesiology and Critical Care Medicine, Johns Hopkins University, Baltimore, Maryland; and <sup>2</sup>Department of Anesthesiology, The First Affiliated Hospital of the University of Science and Technology and Division of Life Sciences and Medicine, University of Science and Technology of China, Hefei, Anhui, China

## Abstract

Endothelial dysfunction is implicated in the thrombotic events reported in patients with coronavirus disease (COVID-19), but the underlying molecular mechanisms are unknown. Circulating levels of the coagulation cascade activator PAI-1 are substantially higher in patients with COVID-19 with severe respiratory dysfunction than in patients with bacterial sepsis and acute respiratory distress syndrome. Indeed, the elevation of PAI-1 is recognized as an early marker of endothelial dysfunction. Here, we report that the rSARS-CoV-2-S1 (recombinant severe acute respiratory syndrome coronavirus 2 [SARS-CoV-2] viral envelope spike) glycoprotein stimulated robust production of PAI-1 by human pulmonary microvascular endothelial cells (HPMECs). We examined the role of protein degradation in this SARS-CoV-2-S1 induction of PAI-1 and found that the proteasomal degradation inhibitor bortezomib inhibited SARS-CoV-2-S1–mediated changes in PAI-1. Our data further show that bortezomib upregulated KLF2, a shear-stress–regulated transcription factor that suppresses PAI-1 expression. Aging and metabolic disorders are known to increase mortality and morbidity in patients with COVID-19. We therefore examined the role of ZMPSTE24 (zinc metalloproteinase STE24), a metalloprotease with a demonstrated role in host defense against RNA viruses that is decreased in older individuals and in metabolic

syndrome, in the induction of PAI-1 in HPMECs by SARS-CoV-2-S1. Indeed, overexpression of ZMPSTE24 blunted enhancement of PAI-1 production in spike protein–exposed HPMECs. In addition, we found that membrane expression of the SARS-CoV-2 entry receptor ACE2 was reduced by ZMPSTE24-mediated cleavage and shedding of the ACE2 ectodomain, leading to accumulation of ACE2 decoy fragments that may bind SARS-CoV-2. These data indicate that decreases in ZMPSTE24 with age and comorbidities may increase vulnerability to vascular endothelial injury by SARS-CoV-2 viruses and that enhanced production of endothelial PAI-1 might play role in prothrombotic events in patients with COVID-19.

**Keywords:** PAI-1; human pulmonary microvascular endothelial cell; zinc metalloproteinase STE24; angiotensin-converting enzyme 2; coronavirus disease

## Clinical Relevance

Findings from current work provide new insights into mechanisms of severe acute respiratory syndrome coronavirus 2 (SARS-CoV-2)–mediated severe acute lung injury and respiratory failure with this infection.

The recent coronavirus disease (COVID-19) pandemic threatens global health and the global economy. To date, severe acute

respiratory syndrome coronavirus 2 (SARS-CoV-2) has infected more than 107 million people and caused more than 2.34 million

deaths worldwide. Most current and planned therapies, including antivirals and vaccines, target viral entry or viral replication (1).

(Received in original form November 30, 2020; accepted in final form April 13, 2021)

This article is open access and distributed under the terms of the Creative Commons Attribution Non-Commercial No Derivatives License 4.0. For commercial usage and reprints, please e-mail Diane Gern.

Supported by an American Heart Association Scientist Development Grant and National Institutes of Health grant R56 HL139736 (D.P.). Dr. Sujatha Kannan, Vice Chair of Research, Department of Anesthesiology and Critical Care Medicine at Johns Hopkins University, provided research funds to support this study.

Author Contributions: Conception and design: M.H. and D.P. Analysis and interpretation: M.H. and D.P. Drafting the manuscript for important intellectual content: M.H. and D.P.

Correspondence and requests for reprints should be addressed to Deepesh Pandey, Ph.D., Department of Anesthesiology and Critical Care Medicine, Johns Hopkins University, 1721 East Madison Street, Ross Building, Room 345, Baltimore, MD 21205. E-mail: dpandey2@jhmi.edu.

This article has a related editorial.

Am J Respir Cell Mol Biol Vol 65, Iss 3, pp 300–308, September 2021

Copyright © 2021 by the American Thoracic Society

Originally Published in Press as DOI: 10.1165/rcmb.2020-0544OC on May 18, 2021

Internet address: www.atsjournals.org

Mortality and infection continue to rise at alarming rates, and therapies to boost innate host defense could offer important alternatives or adjuncts to vaccines and antivirals. Pulmonary microthrombi are prevalent in hospitalized patients with COVID-19, and correlate with disease severity and mortality, yet it is not known whether SARS-CoV-2 modulates host molecular thrombolytic mechanisms (2). We report that production of the critical thrombosis-regulating protein endothelial PAI-1 in human pulmonary microvascular endothelial cells (HPMECs) is induced by SARS-CoV-2-S1 (SARS-CoV-2 viral envelope spike).

PAI-1 is a member of the serine protease inhibitor (serpin) superfamily and is the main physiologic inhibitor of tissue-type plasminogen and urokinase-type plasminogen activator. PAI-1 blocks the conversion of precursor plasminogen to active plasmin (a serine protease involved in the dissolution of fibrin blood clots) (3). A very recent study reported that PAI-1 levels were significantly higher in patients with COVID-19 with severe respiratory dysfunction than in patients with bacterial sepsis and acute respiratory distress syndrome (4). Endothelial cells (ECs) are an important source of circulating PAI-1 (5, 6), and molecules that induce EC injury, such as TNF $\alpha$  (7), TGF $\beta$  (7), AngII (angiotensin II) (8, 9), and thrombin (10), all induce endothelial PAI-1 production. Furthermore, elevated levels of PAI-1 have been implicated in the pathogenesis of several diseases that are caused by endothelial dysfunction (11), including atherosclerosis, endothelial senescence (12–14), and pathologic angiogenesis (15, 16). Interestingly, adipose tissue is the major contributor of circulating PAI-1, and given that obesity is associated with a marked increase in adipocytes, this fact could explain the increased risk for venous thromboembolism, hospitalization, and death due to COVID-19 in patients with obesity (17, 18).

To determine the mechanism underlying enhanced production of PAI-1 in SARS-CoV-2-S1-exposed HPMECs, we examined the impact of proteasomal mediated degradation. In addition, we investigated the role of the ACE2 receptor (angiotensin-converting enzyme 2) in the SARS-CoV-2-S1-mediated activation of HPMECs to produce higher levels of PAI-1. Binding of the S1 glycoprotein to ACE2 on the target cell surface is a common entry mechanism into target cells for the RNA viral family that includes SARS-CoV-2 and Middle East respiratory syndrome coronavirus (19–21). IFITMs (IFN-induced

transmembrane proteins), the innate immune system's first line of defense against viral infection in vertebrates, have been shown to modulate ACE2-mediated entry of SARS-CoV and Middle East respiratory syndrome coronavirus (22–25). Affinity purification coupled with mass spectrometry has enabled identification of ZMPSTE24 (zinc metalloproteinase STE24) as a major binding partner of IFITM3 (26). ZMPSTE24 is a transmembrane metalloprotease with a demonstrated role in host defense against RNA viruses. It is dependent on IFITM (26, 27) and is decreased in cells that are affected by metabolic disorders and aging (28–30). Furthermore, morbidity and mortality from COVID-19 are strikingly higher in older patients and patients with preexisting metabolic diseases (27). ZMPSTE24-deficient mice display higher viral burdens, enhanced cytokine production, and increased mortality after influenza infection (27). Increased susceptibility to viral infection is therefore a likely consequence of insufficient ZMPSTE24 in ECs (31). Therefore, we hypothesized that enhanced SARS-CoV-2 entry into ECs stimulates production of abnormally high levels of endothelial PAI-1 and that strategies for augmentation of ZMPSTE24 expression and activity may provide protection against COVID-19-mediated vascular injury.

We demonstrate that PAI-1 expression is greatly amplified by the spike protein of SARS-CoV-2 viruses in HPMECs and that ZMPSTE24 may be protective against viral entry into these cells. These findings provide clues for amelioration of the devastating thrombotic events that are seen in patients with COVID-19 and may also offer insights regarding the vulnerability of aging individuals with other comorbidities to increased COVID-19 severity.

## Methods

### Reagents and Cell Culture

HPMECs were purchased from Promo Cell. rSARS-CoV-2-S1 (recombinant SARS-CoV-2-S1) protein was purchased from Creative Diagnostics. The ACE2 antibody was purchased from R&D Systems (catalog numbers mab933 and AF933), PAI1 and GAPDH antibodies were purchased from Proteintech, the ZMPSTE24 antibody was purchased from Invitrogen (PA1-16965), the SARS-CoV-2-S1 protein antibody was purchased from Sino Biological, Inc. (catalog number

40591-MM42), and the HA antibody was purchased from Cell Signaling (catalog number 2999S). The lamin A/C antibody was purchased from Santa Cruz Biotechnology (catalog number sc-6215), and the prelamin A antibody was a gift from Dr. Susan Michaelis (Department of Cell Biology, Johns Hopkins University). Unless otherwise stated, all other reagents were obtained from Sigma. HeLa cells were transfected with ACE2 plasmid using Lipofectamine 2000 (Life Technologies) as per the manufacturer protocol. Crispr/Cas9-mediated ZMPSTE24-knockout (KO) HeLa cells were a kind gift from Dr. Fabio Martinon (Department of Biochemistry, University of Lausanne). Cigarette smoke extract was purchased from Murty Pharmaceuticals, and 80  $\mu$ g/ml was added to ECs for 24 hours. Cigarette smoke extract, which consists of 40 mg/ml of smoke condensate and 6% nicotine, was prepared by using a smoke machine to extract smoke from the University of Kentucky's 3R4F Standard Research Cigarettes as per the manufacturer's instructions.

### Generation of Adenoviruses Encoding shRNA

Adenoviruses encoding control scrambled shRNA (sh) and adenoviruses encoding KLF2 shRNA were generated by using a pAdBLOCK-iT kit (Life Sciences). Briefly, oligonucleotides targeting the coding region of human KLF2 and the nontargeted sequence (scrambled) were designed with proprietary software from Life Sciences and cloned into pU6-ENTR vector. Sequences used were as follows: nontargeted: top, 5'-CAC CGA TGG ATT GCA CGC AGG TTC TCG AAA GAA CCT GCG TGC AAT CCA TC-3'; bottom, 5'-AAA AGA TGG ATT GCA CGC AGG TTC TTT CGA GAA CCT GCG TGC AAT CCA TC-3' and KLF2 sh: top, 5'-CAC CGC TGC ACA TGA AAC GGC ACA TCG A-3'; bottom, 5'-AAA AGC TGC ACA TGA AAC GGC ACA TTT C-3'. The resulting pU6-sh-nontargeted and pU6-KLF2 sh plasmids were tested for function in transient transfection experiments with 293A cells. The constructs that showed the greatest inhibition were subjected to *in vitro* recombination with pAD/BLOCK-iTDEST vector (Invitrogen) using Gateway LR clonase enzyme to generate pAd-KLF2 shRNA. Viruses were amplified, purified, and concentrated by using a Millipore kit.

## Adenovirus Production

Adenoviruses encoding HA-tagged KLF2 and KLF2 sh were constructed by subcloning the sequences into entry PENTR1a vector by using restriction enzymes followed by LR recombination with the destination vector PDEST. The resulting PDEST DNA was digested with PacI, ethanol precipitated, and transfected into HEK-293 cells. After a cytopathic effect was achieved, adenoviruses were collected and purified via three freeze–thaw cycles and a Millipore adenovirus purification kit.

## Western Blotting

HPMECs were washed with cold PBS and incubated on ice for 1 hour in cold radioimmunoprecipitation assay lysis buffer (20mM TRIS-HCl at a pH of 7.5, 150mM NaCl, 1mM EDTA, 1mM EGTA, 1% tertigol-type NP40, 1% sodium deoxycholate, 1mM Na<sub>3</sub>VO<sub>4</sub>, 2.5mM sodium pyrophosphate, 1mM β-glycerophosphate, 1 μg/ml of leupeptin, and a 1:1,000-diluted protease inhibitor cocktail from Sigma). Samples were vortexed briefly every 10 minutes. Then, after the remaining tissue was discarded, the samples were sonicated briefly (four times) at power level of 4 and centrifuged at 4°C for 30 minutes at 20,000 × g. Protein in the supernatant was quantified by using a protein quantification assay kit (Bio-Rad). For each sample, 20 μg of protein was combined with 2× Laemmli sample buffer (Bio-Rad), boiled for 5 minutes at 95°C, and separated by using SDS-PAGE. Proteins from conditioned cell culture media were precipitated with chloroform and methanol. Briefly, one-fourth

volume of chloroform and one volume of methanol were added to the media, which was then centrifuged at 13,500 × g for 5 minutes at room temperature. The pellet was air dried, suspended in 1× Laemmli buffer, and then boiled for 5 minutes at 95°C. After electrophoresis, proteins were transferred from the gel onto a polyvinylidene difluoride membrane, which was blocked in 5% milk before being incubated overnight with primary antibodies and then being incubated for 1 hour with secondary antibodies. Protein bands were visualized by using horseradish peroxidase–conjugated secondary antibodies (Invitrogen).

## Lentivirus Production

HA-tagged ZMPSTE24 was cloned into lentiviral vector pLenti-CMV-MCS-GFP-SV-puro, a gift from Paul Odgren (32) (Addgene plasmid number 73582; <http://n2t.net/addgene:73582>; Research Resource Identifier [RRID]: Addgene\_73582), by using an existing ZMPSTE24 construct and directional TOPO cloning (Invitrogen). HEK-293T cells were transfected by using Effectene transfection reagent (Qiagen) together with lentiviral packaging constructs pspax and MD2.G, which were gifts from Didier Trono (Addgene plasmid number 12259; <http://n2t.net/addgene:12259>; RRID: Addgene\_12259). GFP epitope–tagged progerin was a gift from Tom Misteli (33) (Addgene plasmid number 17663; <http://n2t.net/addgene:17663>; RRID: Addgene\_17663). Lentiviral medium was collected after 48 and 72 hours of transfection and then concentrated and purified by using Lenti-X (Takara Bio).

## Statistical Analysis

Statistical significance was determined by using a Student's *t* test or one-way ANOVA as appropriate, with a *post hoc* Tukey test being used for multiple comparisons. Prism 8 software (GraphPad) was used for all calculations. *P* < 0.05 was set as the criterion for statistical significance.

## Results

### rSARS-CoV-2-S1 Stimulates Endothelial PAI-1

Recent reports have shown that patients with COVID-19 have marked endothelial injury and widespread thrombosis (blood clotting), which is associated with severe respiratory failure, multiorgan failure, and increased mortality (34, 35). Endothelial dysfunction is implicated in the thrombotic events reported in patients with COVID-19, but the underlying molecular mechanisms of this devastating complication are unknown. PAI-1 levels are abnormally high in patients with severe COVID-19 and severe respiratory dysfunction (4). Therefore, to determine whether SARS-CoV-2 spike protein infection modulates endothelial PAI-1 expression, we exposed HPMECs to purified rSARS-CoV-2-S1 for 24 hours. After exposure, HPMECs exhibited robust induction of PAI-1 (Figure 1B). An antibody against SARS-CoV-2-S1 protein detected an abundance of spike glycoprotein in the cell lysates (Figure 1A) that increased in a dose-dependent

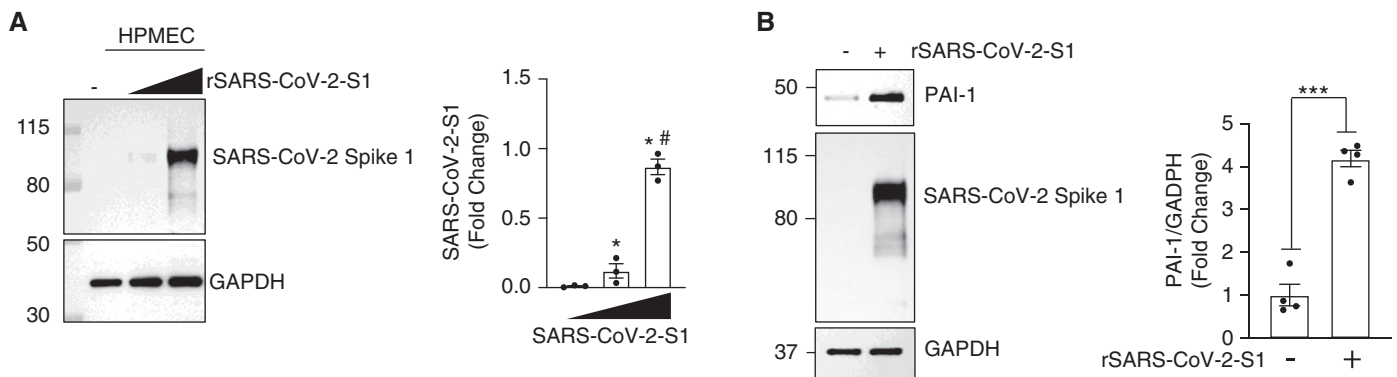


**Figure 1.** SARS-CoV-2-S1 (severe acute respiratory syndrome coronavirus 2 [SARS-CoV-2] viral envelope spike) protein enters human pulmonary microvascular endothelial cells (HPMECs) and robustly increases PAI-1 levels. (A) Lysates from HPMECs that were exposed to 0, 30, or 50 μg of rSARS-CoV-2-S1 (recombinant SARS-CoV-2-S1) protein for 24 hours were immunoblotted with anti-SARS-CoV-2-S1 and anti-GAPDH antibodies. \**P* < 0.05 versus untreated control and #*P* < 0.05 versus 30 μg–treated group (*n* = 3). (B) HPMECs were treated with or without rSARS-CoV-2-S1 protein (50 μg) for 24 hours. Lysates were immunoblotted with anti-PAI-1, anti-SARS-CoV-2-S1, and anti-GAPDH antibodies. \*\*\**P* < 0.001 versus control (PBS) (*n* = 4).

manner, suggesting that recombinant spike protein was able to enter the cells.

**Upregulation of PAI-1 by SARS-CoV-2-S1 Is Dependent on Proteasomal Degradation of the Transcription Factor KLF2**

A previous study suggested that the proteasomal inhibitor bortezomib has thromboprotective effects that are dependent on the transcription factor KLF2 (36). We first tested whether bortezomib could prevent induction of PAI-1 expression by SARS-CoV-2-S1. Strikingly, not only did bortezomib block upregulation of PAI-1 expression, but it also nearly abolished the expression of PAI-1 in these cells (Figure 2A). Furthermore, bortezomib augmented the expression of KLF2 (Figure 2B), which thereby obliterated the expression of PAI-1 in HPMECs (Figure 2C). Overexpression of KLF2 completely blocked the PAI-1 induction mediated by SARS-CoV-2-S1 (Figure 2D), whereas KLF2 silencing by adenovirally delivered

KLF2-specific sh (Figure 2F) increased PAI-1 levels and blocked the downregulation of PAI-1 by bortezomib (Figure 2E). Together, these findings suggest that bortezomib blocks the stimulatory effect of SARS-CoV-2-S1 on PAI-1 expression in lung microvascular endothelium by upregulating the transcriptional regulator KLF2.

**Loss of ZMPSTE24 Preserves Cellular Expression of ACE2 Receptor by Blocking Cleavage Leading to Ectodomain Shedding**

SARS-CoV-2 has been reported to gain entry to cells via the receptor ACE2 (37, 38). To test whether ACE2 is required for recombinant spike protein entry, we incubated HeLa cells with recombinant spike protein, as HeLa cells do not endogenously express ACE2. Interestingly, we detected SARS-CoV-2-S1 in HeLa cell lysates, suggesting that the recombinant spike protein was not solely dependent on ACE2 receptor for entry

(Figure 3). However, rSARS-CoV-2-S1 significantly reduced ACE2 levels in HeLa cells ectopically transfected with ACE2 cDNA (Figure 3). This finding suggests that the rSARS-CoV-2-S1 indeed interacts with ACE2 receptor and reduces its abundance upon entry.

Next, we examined whether downregulation of ZMPSTE24, a critical component of IFITM3-mediated defense against coronaviruses (26, 27), can modulate ACE2 receptor expression. ACE2 ectodomain shedding has been suggested to confer protection against previous coronaviruses (SARS-CoV) by acting as a decoy receptor that binds to the viruses and restricts their entry (39). In ZMPSTE24-KO HeLa cells, the ectopic expression of ACE2 as detected by FLAG antibody was significantly higher than it was in wild-type HeLa cells (Figure 3A). Hence, ZMPSTE24 may cleave the ACE2 ectodomain and promote ACE2 “shedding” (40). Either or both of these processes would explain the low levels of ACE2 expression that we

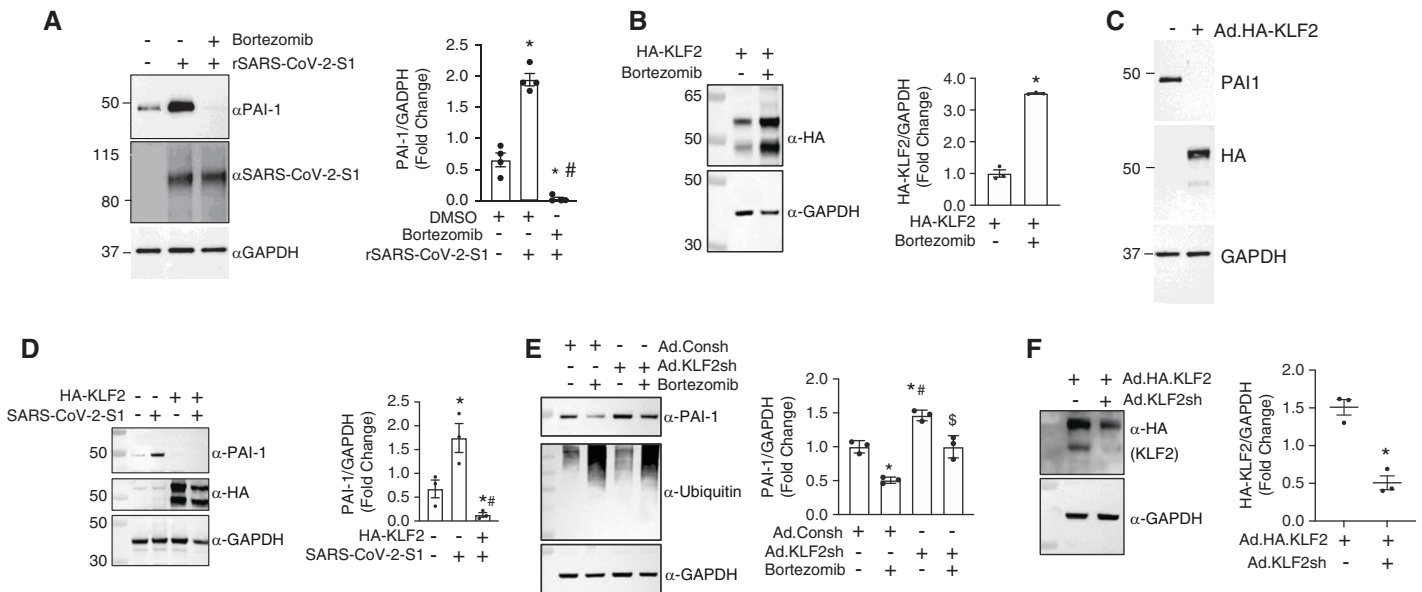


**Figure 2.** SARS-CoV-2-mediated increases in endothelial PAI-1 are completely blocked by the proteasomal inhibitor bortezomib via transcription factor KLF2. (A) HPMECs were incubated with or without rSARS-CoV-2-S1 protein (50 μg, 24 h) in the presence of bortezomib (proteasomal inhibitor) or DMSO (control). Lysates were immunoblotted with anti-PAI-1, anti-SARS-CoV-2-S1, and anti-GAPDH antibodies. \**P* < 0.05 versus DMSO without recombinant spike protein. #*P* < 0.05 versus DMSO with recombinant spike protein (*n* = 4). (B) HPMECs expressing HA epitope-tagged KLF2 were treated with bortezomib or DMSO (control), and cell lysates were immunoblotted with anti-HA and anti-GAPDH antibodies. \**P* < 0.05 versus DMSO (*n* = 3). (C) HPMECs transduced with or without adenoviruses encoding KLF2 were immunoprobed with anti-PAI-1, anti-HA, and anti-GAPDH antibodies (*n* = 3). (D) HPMECs transduced with adenoviruses encoding either empty vector or KLF2 were treated with or without SARS-CoV-2-S1, and cell lysates were immunoblotted with anti-PAI-1, anti-HA, and anti-GAPDH antibodies. \**P* < 0.05 versus untreated cells without KLF2 overexpression and #*P* < 0.05 versus recombinant spike protein with empty vector transduction (*n* = 3). (E) HPMECs transduced with an adenovirus encoding control scrambled shRNA (Ad.Consh) or an adenovirus encoding KLF2 shRNA (Ad.KLF2sh) were treated with bortezomib or DMSO, and cell lysates were immunoblotted with anti-PAI-1, antiubiquitin, and anti-GAPDH antibodies. \**P* < 0.05 versus DMSO and Ad.Consh. #*P* < 0.05 versus bortezomib and Ad.Consh. \$*P* < 0.05 versus DMSO with Ad.KLF2sh (*n* = 3). (F) HPMECs overexpressing HA epitope-tagged KLF2 were transduced with either Ad.Consh or Ad.KLF2sh, and cell lysates were immunoblotted after 72 hours with anti-HA and anti-GAPDH antibodies. \**P* < 0.05 versus Ad.Consh (*n* = 3). Ad.HA.KLF2 = adenovirus encoding HA-KLF2.

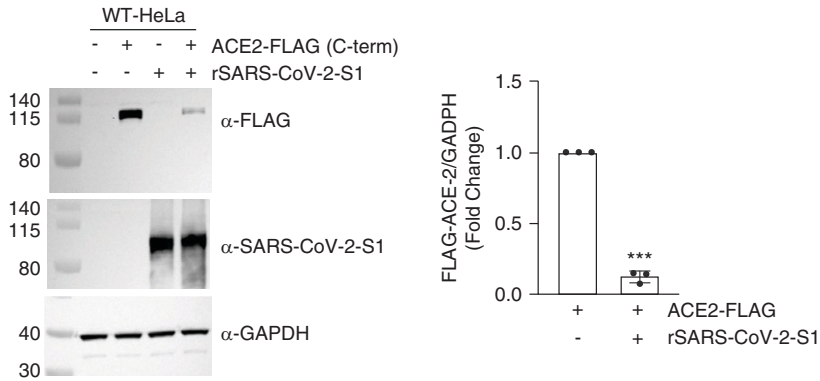


**Figure 3.** rSARS-CoV-2-S1 effects on ACE2 (angiotensin-converting enzyme 2) receptor expression are analogous to the live viral effect. HeLa cells were transfected with ACE2-FLAG and incubated with or without rSARS-CoV 2-S1. IB data from probing with anti-FLAG, anti-SARS-CoV-2-S1, and anti-GAPDH antibodies are shown. \*\*\* $P < 0.001$  versus ACE2-FLAG expression in wild-type (WT) HeLa cells ( $n = 3$ ).

detect in cell lysates of wild-type HeLa cells (with normal levels of ZMPSTE24). Indeed, we found abundant ACE2 levels in conditioned media of ACE2-transfected wild-type HeLa cells and nearly no ACE2 in ACE2-transfected ZMPSTE24-KO HeLa cells using antibodies raised against the N-terminal ectodomain of ACE2 (Figure 4B). Furthermore, the ectodomain antibody also detected a cleaved ACE2 species in wild-type HeLa cells that was absent in ZMPSTE24-KO HeLa cells (Figure 4C). Interestingly, the cleavage site for ACE2 shedding (39) has a high degree of homology with the ZMPSTE24 cleavage site in prelamin A (28). Identical features include two leucine residues at the cleavage site and an arginine residue that occurs

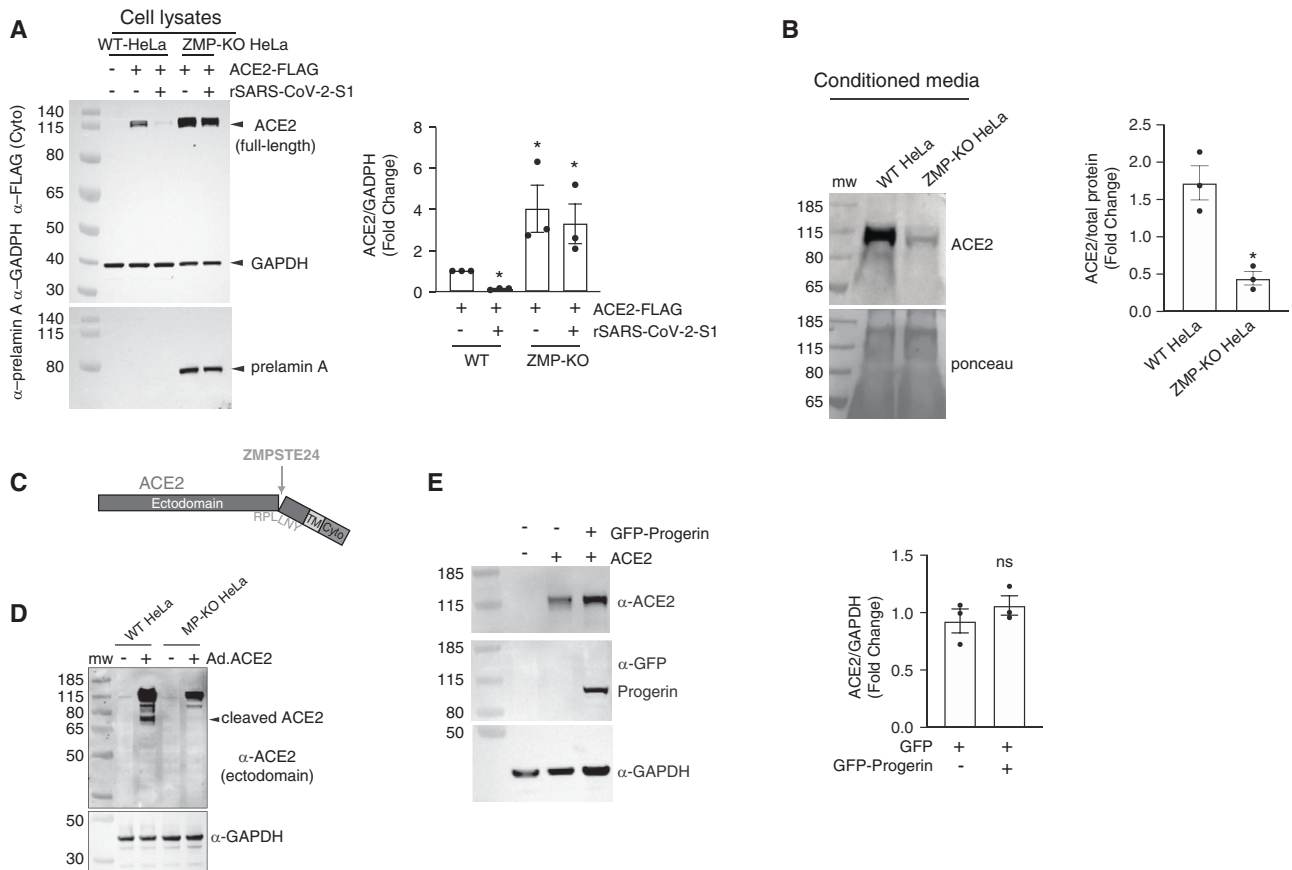


**Figure 4.** ZMPSTE24 (zinc metalloproteinase STE24) is critical for ACE2 cellular expression. (A) Normal (WT) and ZMPSTE24-knockout (ZMP-KO) HeLa cells were transfected with or without ACE2 (C-terminal FLAG-tagged) plasmid and treated with or without rSARS-CoV-2-S1 protein. Cell lysates were immunoblotted with anti-ACE2, anti-FLAG, and anti-GAPDH antibodies. \* $P < 0.05$  versus ACE2-expressing WT HeLa cells ( $n = 3$ ). (B) Conditioned media from WT or ZMP-KO HeLa cells transfected with FLAG-ACE2 were immunoblotted with ectodomain-specific anti-ACE2 antibody and stained with ponceau to determine total protein loading. \* $P < 0.05$  versus ACE2-expressing WT HeLa cells ( $n = 3$ ). (C) Schematic of ACE2 depicts the N-terminal ectodomain, TM domain, and Cyto domain. Leucine584 is a potential ZMPSTE24 cleavage site (RPLLNYF). (D) WT and ZMP-KO HeLa cells were transfected with adenoviruses encoding ACE2, and cell lysates were immunoblotted with ectodomain-specific anti-ACE2 and anti-GAPDH antibodies ( $n = 3$ ). (E) WT HeLa cells cotransfected with either ACE2 and GFP (control) or ACE2 and GFP-tagged progerin were immunoblotted with ectodomain-specific anti-ACE2, anti-GFP, and anti-GAPDH antibodies ( $n = 3$ ). Cyto = cytoplasmic; ns = not statistically significant; TM = transmembrane.

three residues earlier (Figures 4C and 5A). To determine whether the effects of ZMPSTE24 deletion on ACE2 levels are mediated by the accumulation of unprocessed prelamins A, a previously known substrate of ZMPSTE24, we conducted experiments to test the effect of

progerin (internally deleted form of prelamins A) overexpression on ACE2 levels in HeLa cells cotransfected with either ACE2 and GFP (control) or ACE2 and GFP-tagged progerin. We found no significant differences in ACE2 levels between these conditions (Figure 4E).

### ZMPSTE24 Function Declines in HPMECs after Exposure to Injury from Cigarette Smoke Extract and with Aging

We were intrigued by reports that a greater severity of COVID-19 and higher rates of death were correlated with older age and comorbidities such as cigarette smoking. ZMPSTE24 has been shown to defend against enveloped RNA viruses like SARS-CoV-2, and studies indicate that loss of ZMPSTE24 function can lead to premature aging syndromes (progeria) (31). We found that HPMECs exposed to cigarette smoke extract, a well-described injury stimulus for lung and endothelial injury, significantly decreased ZMPSTE24 expression and concomitantly increased unprocessed prelamins A (Figures 5A and 5B). Furthermore, in an *in vitro* model of EC aging, prelamins A accumulated in high-passage (passage 10) ECs, indicating a decline in ZMPSTE24-mediated cleavage (data not shown).

### ZMPSTE24 Attenuates SARS-CoV-2-S1-induced PAI-1 Production by HPMECs

We hypothesized that declining abundance and/or function of endothelial ZMPSTE24 could decrease the ability of ECs to defend against SARS-CoV-2 viral entry and its consequences, including enhanced expression of the procoagulant gene product PAI-1. Indeed, overexpression of ZMPSTE24 in HPMECs via lentivirally mediated gene delivery significantly blocked the SARS-CoV-2-S1-mediated induction of PAI-1 (Figure 6).

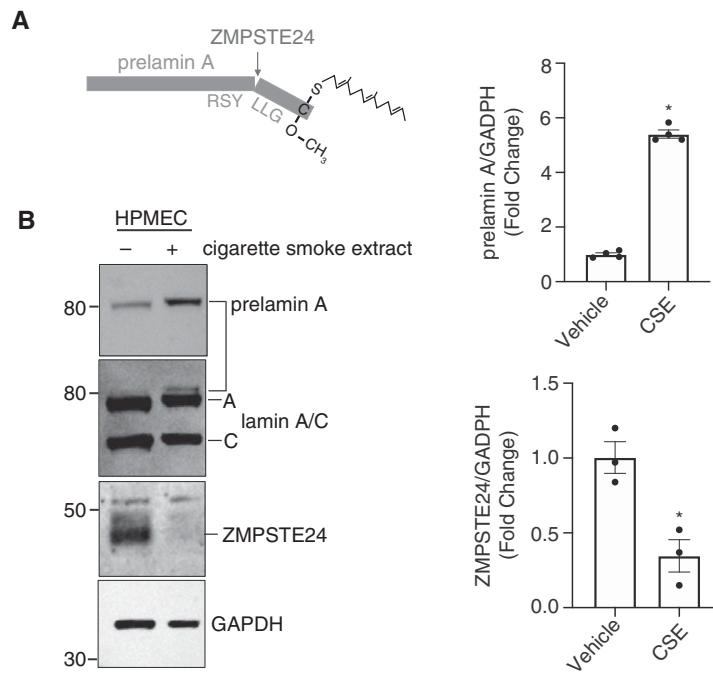


**Figure 5.** Exposure of HPMECs to cigarette smoke extract (CSE) decreases ZMPSTE24 abundance and function. (A) Schematic of prelamins A cleavage by ZMPSTE24. (B) Immunoblot of HPMECs cultured with or without CSE. \* $P < 0.05$  versus vehicle for both high prelamins A and low ZMPSTE24 in cells exposed to CSE ( $n = 3$ ).

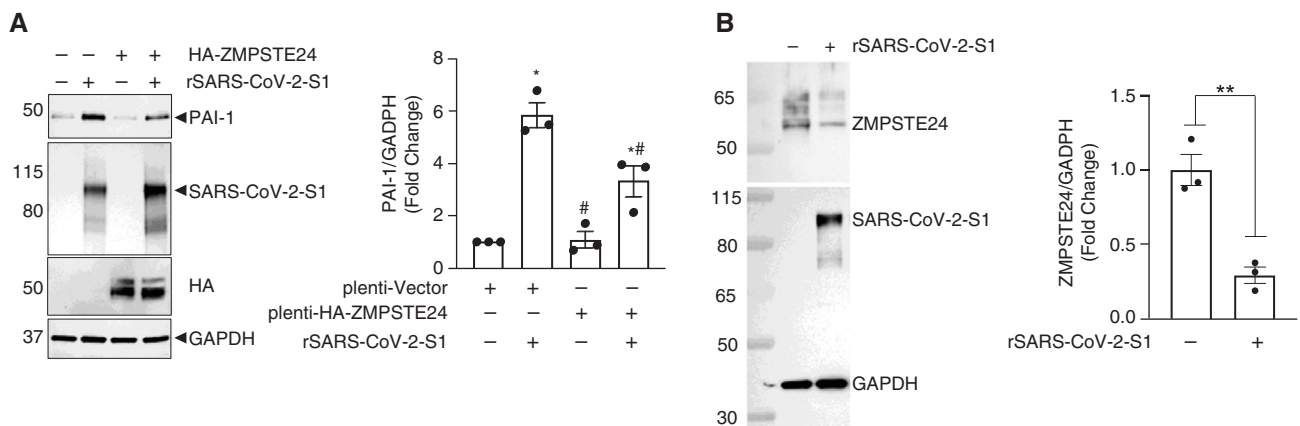


**Figure 6.** Upregulation of PAI-1 by SARS-CoV-2-S1 is dependent on ZMPSTE24. (A) HPMECs that lacked or overexpressed lentivirally mediated HA-tagged ZMPSTE24 were exposed to rSARS-CoV-2-S1 protein (50 μg, 24 h). Lysates were then immunoblotted with anti-PAI-1, anti-HA, anti-SARS-CoV-2-S1, and anti-GAPDH antibodies. \* $P < 0.05$  versus plenti-Vector and # $P < 0.05$  versus plenti-HA-ZMPSTE24 ( $n = 3$ ). (B) Lysates from HPMECs that were exposed to 50 μg of rSARS-CoV-2-S1 protein for 24 hours were immunoblotted with anti-ZMPSTE24, anti-SARS-CoV-2-S1, and anti-GAPDH antibodies. \*\* $P < 0.01$  versus untreated control ( $n = 3$ ).

Intriguingly, SARS-CoV-2-S1 levels were higher in ZMPSTE24-overexpressing cells, although the expression of PAI-1 induced by SARS-CoV-2-S1 was blunted. We therefore examined whether SARS-CoV-2-S1 decreased ZMPSTE24 levels. Indeed, we found significantly reduced ZMPSTE24 expression in HPMECs exposed to SARS-CoV-2-S1 (Figure 6B).

## Discussion

In this study, we found that rSARS-CoV-2-S1 crossed the HPMEC plasma membrane barrier and elicited cellular responses, including augmentation of PAI-1 production. Interestingly, the stimulatory effect of spike protein on endothelial PAI-1 production was completely blocked by bortezomib, a proteasome inhibitor that blocks ubiquitin-mediated protein degradation. Our data further suggest that the KLF2 transcription factor is a potential target of bortezomib in blocking the effect of rSARS-CoV-2-S1; bortezomib robustly increased KLF2 levels, and KLF2 overexpression obviated the increase in PAI-1 levels in HPMECs that were exposed to SARS-CoV-2-S1. This finding is supported by a previous study, which suggested that thromboprotective effects of bortezomib may be dependent on KLF2 (36).

Our data further indicate that SARS-CoV-2-S1 obliterated membrane expression of the ACE2 receptor and that this is mediated by ZMPSTE24. ZMPSTE24 has an established role in defending eukaryotic cells from RNA viruses. In addition, ZMPSTE24 is negatively regulated by cigarette smoke extract, an injury stimulus that causes endothelial dysfunction and lung injury. Finally, increased expression of ZMPSTE24 attenuated spike protein-triggered overproduction of PAI-1 in HPMECs.

Accumulating evidence suggests that enhanced widespread intravascular coagulation and intussusceptive angiogenesis leading to local hypoxia are major contributors to disease severity and mortality from COVID-19. Although EC injury has been proposed as a mechanism for increased clotting, specific EC targets have not yet been described. In our study, we showed that rSARS-CoV-2-S1 was sufficient to activate PAI-1 synthesis in lung microvascular ECs. ECs are a major source of circulating PAI-1, which inhibits processes that lyse blood clots.

Thus, the fourfold increase in PAI-1 that we report here is of great interest. Elevated PAI-1 levels can cause endothelial dysfunction (11) and lung injury by inducing cellular senescence (12–14) and thereby promoting local hypoxia (15, 16).

It is unclear whether the augmentation of PAI-1 was mediated through the ACE2 receptor. When we attempted to address this question by silencing the ACE2 gene with an siRNA approach, we were surprised to find that ACE2 endogenous expression was almost undetectable in quiescent HPMEC lysates, despite our use of two different specific antibodies that were highly effective in detecting ACE2 in HeLa cells transfected with ACE2 plasmid (Figure 5A). Notably, the expression of ACE2 was robust in ZMPSTE24-KO HeLa cells. This finding suggests that the absence of ZMPSTE24 preserved the presence of ACE2 receptor in the cell membrane. The predicted ectodomain consensus sequence of ACE2 is strikingly similar to the ZMPSTE24 cleavage sequence in prelamin A. This similarity suggests that ZMPSTE24 catalyzes ACE2 cleavage and triggers its secretion from ECs. The secreted ACE2, which lacks a transmembrane domain

and cytoplasmic tail, could act as a decoy for SARS-CoV-2 virus and prevent viral entry and injury to HPMECs (Figure 7) (40).

Deletion of ZMPSTE24, a protease responsible for nuclear scaffold prelamin A cleavage and maturation, causes accumulation of unprocessed prelamin A and misshapen nuclei (41, 42). Studies also indicate that a loss-of-function mutation in ZMPSTE24 can lead to premature aging syndromes (progeria) (31). Intriguingly, patients with premature aging syndromes have severe metabolic syndrome (lipodystrophy and low leptin levels), spine curvature (kyphosis), profuse weight and hair loss, and accelerated atherosclerosis that causes death in the early teen years from heart disease (28–30). Furthermore, ZMPSTE24 expression has been shown to decline with aging (43), and patients with a ZMPSTE24 mutation present with hypertriglyceridemia, early onset of type 2 diabetes, and obesity (30). It is notable that in a COVID-19 model produced by infecting Syrian hamsters with live SARS-CoV-2, the hamsters exhibited a very similar phenotype to that of ZMPSTE24-KO mice or a prematurely aging patient (i.e., progressive weight loss, hunched posture, and ruffled hair or fur). This evidence further

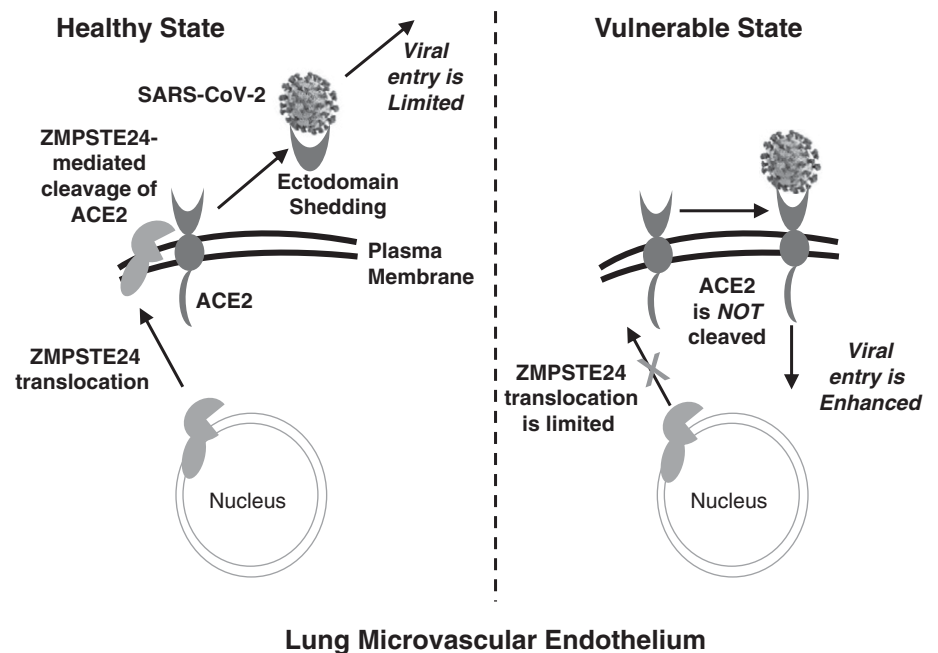


**Figure 7.** Proposed molecular mechanism for enhanced SARS-CoV-2 viral entry and pathogenesis in the pulmonary microcirculation. In the healthy state (left), ZMPSTE24 cleaves the ACE2 receptor on the endothelial cell surface, thereby facilitating ACE2 ectodomain shedding and restricting viral entry. In the vulnerable state (right), comorbidities may reduce expression and/or trafficking of ZMPSTE24 to the plasma membrane. The reduction in ZMPSTE24 limits ACE2 shedding, thereby increasing lung microvascular vulnerability to SARS-CoV-2 and subsequent induction of PAI-1.

strengthens our hypothesis that ZMPSTE24 function is critical to EC defense against COVID-19. One limitation of our study is that we still do not know whether accumulated unprocessed prelamin A played any role in enhancing ACE2 levels and reversing the S1-mediated ACE2 downregulation in cells with ZMPSTE24 deletion. We examined the effect of progerin, a splice mutant of prelamin A that causes classical progeria syndrome, on ACE2 expression and found no significant effect. Hence, the effects of ZMPSTE24 on ACE2 appear to be independent of unprocessed lamin A. However, this aberrant splicing form of prelamin A may occur only rarely in an individual without disease. Therefore, additional studies are needed that use unprocessed and permanently farnesylated prelamin A (an uncleavable form of lamin A, Leucine648 to Arginine mutant) as a trigger for enhanced ACE2 levels in ZMPSTE24-KO cells.

SARS-CoV-2 is believed to enter cells via the ACE2 receptor. We found that rSARS-CoV-2-S1 significantly reduced ACE2 expression in HeLa cells that had been

ectopically transfected with ACE2 cDNA. This phenomenon has also been described with the previous coronaviruses (SARS-CoV) that use ACE2 receptor for cell entry (40, 44). The reduction in ACE2 could explain the compromised lung function of patients with COVID-19, as ACE2 has been reported to protect against acute lung injury in several models of acute respiratory distress syndrome. ACE2 exerts its protective effect by degrading AngII to angiotensin 1–7. AngII triggers many adverse effects, including increased coagulation, endothelial dysfunction, oxidative stress, inflammation, hypertension, lung injury, fibrosis, and pulmonary hypertension (45–48). Downregulation of ACE2 by SARS-CoV-2-S1 provides evidence that this protein is intrinsic to the endothelial injury described in the lungs of patients with COVID-19. ACE inhibition with ramipril has been shown to decrease plasma levels of PAI-1 and may find use as an adjunctive therapy to attenuate the induction of PAI-1 by SARS-CoV-2.

In summary, our findings yield new insights into the mechanisms by which SARS-CoV-2 infects lung tissue (Figure 7). The

pathogenesis of severe acute lung injury and respiratory failure with COVID-19 suggests a quantifiable means for assaying vulnerability to these severe manifestations in key target subpopulations. Our results also imply that bortezomib may be repurposed from existing therapeutics (for multiple myeloma) to blunt complications from intravascular coagulation and endothelial dysfunction and hasten recovery from SARS-CoV-2 and similar infections. Pharmacologic inhibitors of PAI-1, such as PAI-039 and MDI-2268, have been shown to inhibit atherosclerosis in mice with obesity and metabolic syndrome (49). Future studies are warranted to determine whether PAI-1 inhibitors could ameliorate thromboembolism and mortality in patients with COVID-19. ■

**Author disclosures** are available with the text of this article at [www.atsjournals.org](http://www.atsjournals.org).

**Acknowledgment:** The authors thank Claire Levine, M.S., E.L.S., Scientific Editor in the Department of Anesthesiology and Critical Care Medicine at Johns Hopkins University, for editing this manuscript.

## References

- Wang M, Cao R, Zhang L, Yang X, Liu J, Xu M, *et al*. Remdesivir and chloroquine effectively inhibit the recently emerged novel coronavirus (2019-nCoV) *in vitro*. *Cell Res* 2020;30:269–271.
- Zhou F, Yu T, Du R, Fan G, Liu Y, Liu Z, *et al*. Clinical course and risk factors for mortality of adult inpatients with COVID-19 in Wuhan, China: a retrospective cohort study. *Lancet* 2020;395:1054–1062.
- Kruithof EK, Tran-Thang C, Bachmann F. The fast-acting inhibitor of tissue-type plasminogen activator in plasma is also the primary plasma inhibitor of urokinase. *Thromb Haemost* 1986;55:65–69.
- Kang S, Tanaka T, Inoue H, Ono C, Hashimoto S, Kioi Y, *et al*. IL-6 trans-signaling induces plasminogen activator inhibitor-1 from vascular endothelial cells in cytokine release syndrome. *Proc Natl Acad Sci USA* 2020;117:22351–22356.
- Levin EG. Quantitation and properties of the active and latent plasminogen activator inhibitors in cultures of human endothelial cells. *Blood* 1986;67:1309–1313.
- Loskutoff DJ, van Mourik JA, Erickson LA, Lawrence D. Detection of an unusually stable fibrinolytic inhibitor produced by bovine endothelial cells. *Proc Natl Acad Sci USA* 1983;80:2956–2960.
- Sawdey M, Podor TJ, Loskutoff DJ. Regulation of type 1 plasminogen activator inhibitor gene expression in cultured bovine aortic endothelial cells. Induction by transforming growth factor-beta, lipopolysaccharide, and tumor necrosis factor-alpha. *J Biol Chem* 1989;264:10396–10401.
- Ridker PM, Gaboury CL, Conlin PR, Seely EW, Williams GH, Vaughan DE. Stimulation of plasminogen activator inhibitor *in vivo* by infusion of angiotensin II. Evidence of a potential interaction between the renin-angiotensin system and fibrinolytic function. *Circulation* 1993;87:1969–1973.
- Vaughan DE, Lazos SA, Tong K. Angiotensin II regulates the expression of plasminogen activator inhibitor-1 in cultured endothelial cell: a potential link between the renin-angiotensin system and thrombosis. *J Clin Invest* 1995;95:995–1001.
- Heaton JH, Dame MK, Gelehrter TD. Thrombin induction of plasminogen activator inhibitor mRNA in human umbilical vein endothelial cells in culture. *J Lab Clin Med* 1992;120:222–228.
- Ross R. The pathogenesis of atherosclerosis: an update. *N Engl J Med* 1986;314:488–500.
- Serrano M, Lin AW, McCurrach ME, Beach D, Lowe SW. Oncogenic ras provokes premature cell senescence associated with accumulation of p53 and p16INK4a. *Cell* 1997;88:593–602.
- Comi P, Chiaramonte R, Maier JA. Senescence-dependent regulation of type 1 plasminogen activator inhibitor in human vascular endothelial cells. *Exp Cell Res* 1995;219:304–308.
- Vaughan DE, Rai R, Khan SS, Eren M, Ghosh AK. Plasminogen activator inhibitor-1 is a marker and a mediator of senescence. *Arterioscler Thromb Vasc Biol* 2017;37:1446–1452.
- Isogai C, Laug WE, Shimada H, Declerck PJ, Stins MF, Durden DL, *et al*. Plasminogen activator inhibitor-1 promotes angiogenesis by stimulating endothelial cell migration toward fibronectin. *Cancer Res* 2001;61:5587–5594.
- Mimuro J, Schleeff RR, Loskutoff DJ. Extracellular matrix of cultured bovine aortic endothelial cells contains functionally active type 1 plasminogen activator inhibitor. *Blood* 1987;70:721–728.
- Sawdey MS, Loskutoff DJ. Regulation of murine type 1 plasminogen activator inhibitor gene expression *in vivo*: tissue specificity and induction by lipopolysaccharide, tumor necrosis factor-alpha, and transforming growth factor-beta. *J Clin Invest* 1991;88:1346–1353.
- Hendren NS, de Lemos JA, Ayers C, Das SR, Rao A, Carter S, *et al*. Association of body mass index and age with morbidity and mortality in patients hospitalized with COVID-19: results from the American Heart Association COVID-19 cardiovascular disease registry. *Circulation* 2021;143:135–144.
- Zhang H, Penninger JM, Li Y, Zhong N, Slutsky AS. Angiotensin-converting enzyme 2 (ACE2) as a SARS-CoV-2 receptor: molecular mechanisms and potential therapeutic target. *Intensive Care Med* 2020;46:586–590.
- Li W, Zhang C, Sui J, Kuhn JH, Moore MJ, Luo S, *et al*. Receptor and viral determinants of SARS-coronavirus adaptation to human ACE2. *EMBO J* 2005;24:1634–1643.

21. Hoffmann M, Kleine-Weber H, Schroeder S, Krüger N, Herrler T, Erichsen S, *et al.* SARS-COV-2 cell entry depends on ACE2 and TMPRSS2 and is blocked by a clinically proven protease inhibitor. *Cell* 2020;181:271–280, e8.
22. Cullen BR, Cherry S, tenOever BR. Is RNA interference a physiologically relevant innate antiviral immune response in mammals? *Cell Host Microbe* 2013;14:374–378.
23. Chang J, Block TM, Guo JT. The innate immune response to hepatitis B virus infection: implications for pathogenesis and therapy. *Antiviral Res* 2012;96:405–413.
24. Diamond MS, Farzan M. The broad-spectrum antiviral functions of IFIT and IFITM proteins. *Nat Rev Immunol* 2013;13:46–57.
25. Bailey CC, Zhong G, Huang IC, Farzan M. IFITM-family proteins: the cell's first line of antiviral defense. *Annu Rev Virol* 2014;1:261–283.
26. Li S, Fu B, Wang L, Dorf ME. ZMPSTE24 is downstream effector of interferon-induced transmembrane antiviral activity. *DNA Cell Biol* 2017;36:513–517.
27. Fu B, Wang L, Li S, Dorf ME. ZMPSTE24 defends against influenza and other pathogenic viruses. *J Exp Med* 2017;214:919–929.
28. Wang Y, Lichter-Konecki U, Anyane-Yeboah K, Shaw JE, Lu JT, Östlund C, *et al.* A mutation abolishing the ZMPSTE24 cleavage site in prelamin A causes a progeroid disorder. *J Cell Sci* 2016;129:1975–1980.
29. Worman HJ, Michaelis S. Permanently farnesylated prelamin a, progeria, and atherosclerosis. *Circulation* 2018;138:283–286.
30. Galant D, Gaborit B, Desgrouais C, Abdesselam I, Bernard M, Levy N, *et al.* A heterozygous ZMPSTE24 mutation associated with severe metabolic syndrome, ectopic fat accumulation, and dilated cardiomyopathy. *Cells* 2016;5:21.
31. Spear ED, Hsu ET, Nie L, Carpenter EP, Hrycyna CA, Michaelis S. ZMPSTE24 missense mutations that cause progeroid diseases decrease prelamin A cleavage activity and/or protein stability. *Dis Model Mech* 2018;11:dmm033670.
32. Witwicka H, Hwang SY, Reyes-Gutierrez P, Jia H, Odgren PE, Donahue LR, *et al.* Studies of OC-STAMP in osteoclast fusion: a new knockout mouse model, rescue of cell fusion, and transmembrane topology. *PLoS One* 2015;10:e0128275.
33. Scaffidi P, Misteli T. Lamin A-dependent misregulation of adult stem cells associated with accelerated ageing. *Nat Cell Biol* 2008;10:452–459.
34. Ackermann M, Verleden SE, Kuehnel M, Haverich A, Welte T, Laenger F, *et al.* Pulmonary vascular endothelialitis, thrombosis, and angiogenesis in COVID-19. *N Engl J Med* 2020;383:120–128.
35. Rapkiewicz AV, Mai X, Carsons SE, Pittaluga S, Kleiner DE, Berger JS, *et al.* Megakaryocytes and platelet-fibrin thrombi characterize multi-organ thrombosis at autopsy in COVID-19: a case series. *EClinicalMedicine* 2020;24:100434.
36. Nayak L, Shi H, Atkins GB, Lin Z, Schmaier AH, Jain MK. The thromboprotective effect of bortezomib is dependent on the transcription factor Kruppel-like factor 2 (KLF2). *Blood* 2014;123:3828–3831.
37. Sampaio WO, Henrique de Castro C, Santos RA, Schiffrin EL, Touyz RM. Angiotensin-(1-7) counterregulates angiotensin II signaling in human endothelial cells. *Hypertension* 2007;50:1093–1098.
38. Sampaio WO, Souza dos Santos RA, Faria-Silva R, da Mata Machado LT, Schiffrin EL, Touyz RM. Angiotensin-(1-7) through receptor Mas mediates endothelial nitric oxide synthase activation via Akt-dependent pathways. *Hypertension* 2007;49:185–192.
39. Jia HP, Look DC, Tan P, Shi L, Hickey M, Gakhar L, *et al.* Ectodomain shedding of angiotensin converting enzyme 2 in human airway epithelia. *Am J Physiol Lung Cell Mol Physiol* 2009;297:L84–L96.
40. Glowacka I, Bertram S, Herzog P, Pfefferle S, Steffen I, Muench MO, *et al.* Differential downregulation of ACE2 by the spike proteins of severe acute respiratory syndrome coronavirus and human coronavirus NL63. *J Virol* 2010;84:1198–1205.
41. Bergo MO, Gavino B, Ross J, Schmidt WK, Hong C, Kendall LV, *et al.* Zmpste24 deficiency in mice causes spontaneous bone fractures, muscle weakness, and a prelamin A processing defect. *Proc Natl Acad Sci USA* 2002;99:13049–13054.
42. Young SG, Meta M, Yang SH, Fong LG. Prelamin A farnesylation and progeroid syndromes. *J Biol Chem* 2006;281:39741–39745.
43. Ragnauth CD, Warren DT, Liu Y, McNair R, Tajsic T, Figg N, *et al.* Prelamin A acts to accelerate smooth muscle cell senescence and is a novel biomarker of human vascular aging. *Circulation* 2010;121:2200–2210.
44. Kuba K, Imai Y, Rao S, Gao H, Guo F, Guan B, *et al.* A crucial role of angiotensin converting enzyme 2 (ACE2) in SARS coronavirus-induced lung injury. *Nat Med* 2005;11:875–879.
45. Ferreira AJ, Shenoy V, Yamazato Y, Sriramula S, Francis J, Yuan L, *et al.* Evidence for angiotensin-converting enzyme 2 as a therapeutic target for the prevention of pulmonary hypertension. *Am J Respir Crit Care Med* 2009;179:1048–1054.
46. Yamazato Y, Ferreira AJ, Hong KH, Sriramula S, Francis J, Yamazato M, *et al.* Prevention of pulmonary hypertension by angiotensin-converting enzyme 2 gene transfer. *Hypertension* 2009;54:365–371.
47. Rabelo LA, Xu P, Todiras M, Sampaio WO, Buttgerit J, Bader M, *et al.* Ablation of angiotensin (1-7) receptor Mas in C57Bl/6 mice causes endothelial dysfunction. *J Am Soc Hypertens* 2008;2:418–424.
48. Rentzsch B, Todiras M, Iliescu R, Popova E, Campos LA, Oliveira ML, *et al.* Transgenic angiotensin-converting enzyme 2 overexpression in vessels of SHRSP rats reduces blood pressure and improves endothelial function. *Hypertension* 2008;52:967–973.
49. Khoukaz HB, Ji Y, Braet DJ, Vadali M, Abdelhamid AA, Emal CD, *et al.* Drug targeting of plasminogen activator inhibitor-1 inhibits metabolic dysfunction and atherosclerosis in a murine model of metabolic syndrome. *Arterioscler Thromb Vasc Biol* 2020;40:1479–1490.